



**Synthesis and Characterization of Multipod Frameworks of  
Cu<sub>2</sub>O Microcrystals and Cu<sub>7</sub>S<sub>4</sub> Hollow Microcages**

Journal:	<i>CrystEngComm</i>
Manuscript ID:	CE-COM-02-2015-000286.R1
Article Type:	Communication
Date Submitted by the Author:	10-Mar-2015
Complete List of Authors:	Zhang, Hongdan; Jilin University, State Key Lab of Inorganic Synthesis and Preparative Chemistry Zhang, Ziqing; Jilin University, State Key Lab of Inorganic Synthesis and Preparative Chemistry Li, Benxian; Jilin University, College of earth science Hua, Yingjie; Hainan Normal University, School of Chemistry and Chemical Engineering Wang, Chongtai; Hainan Normal University, School of Chemistry and Chemical Engineering Zhao, Xudong; Jilin University, State Key Lab of Inorganic Synthesis and Preparative Chemistry Liu, Xiaoyang; Jilin University, State Key Lab of Inorganic Synthesis and Preparative Chemistry

## COMMUNICATION

## Synthesis and Characterization of Multipod Frameworks of Cu<sub>2</sub>O Microcrystals and Cu<sub>7</sub>S<sub>4</sub> Hollow Microcages

Cite this: DOI: 10.1039/x0xx00000x

Hongdan Zhang,<sup>a</sup> Ziqing Zhang,<sup>a</sup> Benxian Li,<sup>b</sup> Yingjie Hua,<sup>c</sup> Chongtai Wang,<sup>c</sup>  
Xudong Zhao<sup>a\*</sup> and Xiaoyang Liu<sup>a\*</sup>

Received 00th January 2012,  
Accepted 00th January 2012

DOI: 10.1039/x0xx00000x

www.rsc.org/

**A variety of multipod frameworks of Cu<sub>2</sub>O microcrystals have been prepared through careful control of the ratios of n-butyl alcohol to water. And novel 14-pods Cu<sub>2</sub>O frameworks are first reported. Moreover, a template-assisted synthesis of multipod frameworks of Cu<sub>7</sub>S<sub>4</sub> microcages using the obtained Cu<sub>2</sub>O microcrystals as sacrificial templates is reported.**

Architectural control of inorganic materials with well-defined shapes have attracted increasing interest due to their unique shape-dependent physical and chemical properties.<sup>1</sup> In recent years, considerable attention has been focused on the various polyhedron-based dendrites or branched structures.<sup>2–12</sup> For example, PbS star-shaped nanocrystals, multipods and dendrites,<sup>2–4</sup> MnO multipods,<sup>5–7</sup> flower-shaped Ag<sub>2</sub>O particles,<sup>8</sup> and branched Cu<sub>2</sub>O crystals<sup>9–12</sup> from nanometer to micrometer sizes have been prepared.

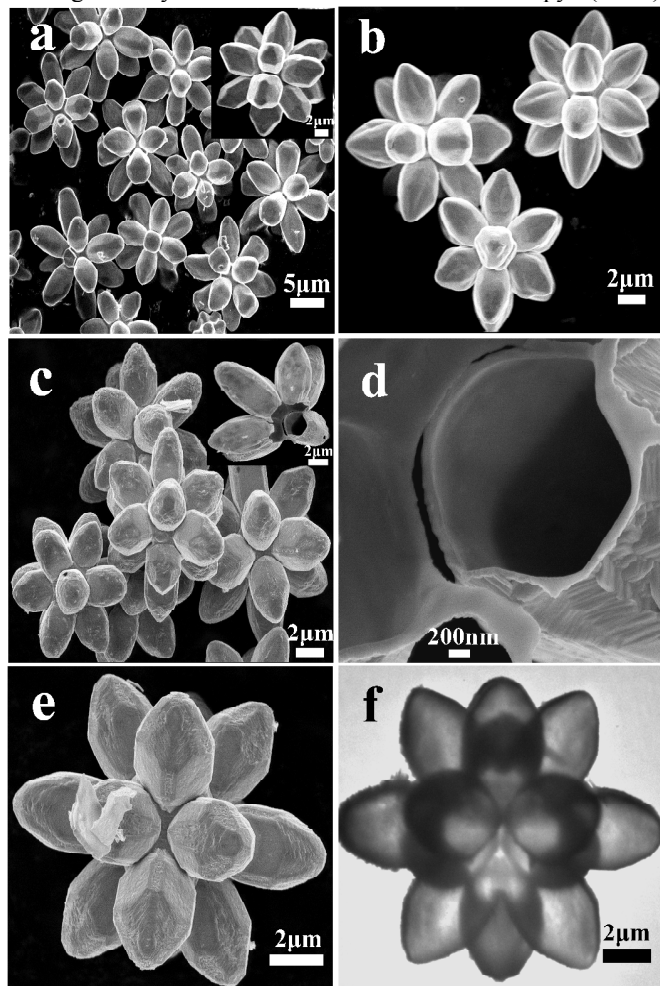
Cuprous oxide (Cu<sub>2</sub>O), as a representative p-type semiconductor with a band gap of 2.17 eV, has been widely investigated for its potential applications in solar energy conversion,<sup>13</sup> electrodes of lithium ion batteries,<sup>14</sup> gas sensing<sup>15</sup> and photocatalytic degradation of organic pollutants.<sup>16–20</sup> It is meaningful to investigate the morphological evolution of Cu<sub>2</sub>O, especially the multipod-shaped microcrystals, which can provide important information to the fields of crystal growth, design, and morphology-controlled synthesis of Cu<sub>2</sub>O, and further other inorganic building blocks. Many methods have been developed to prepare multipod-shaped of Cu<sub>2</sub>O microcrystal.<sup>21–29</sup> Choi et al. prepared multipod-shaped Cu<sub>2</sub>O crystals by tuning the deployed synthetic parameters (pH, temperature and concentration) in their electrodeposition processes.<sup>21, 22</sup> Liu et al. synthesized hexapod-shaped Cu<sub>2</sub>O microcrystals via a  $\gamma$ -irradiation reduction route.<sup>23</sup> However, the development of facile, rapid, and green methods for fabricating Cu<sub>2</sub>O with multipod-shaped remains a key scientific challenge.

Herein, we present a rational synthetic scheme that yields novel multipod frameworks of Cu<sub>2</sub>O microcrystals in a model study of the shape-guiding strategy. A series of Cu<sub>2</sub>O multipod frameworks have been synthesized by adding weak reductive agent EDTANa<sub>2</sub>·2H<sub>2</sub>O into CuAc<sub>2</sub>·2H<sub>2</sub>O solution and varying the volume ratios of n-butyl alcohol to water in the reaction

solvent. Most rewardingly, novel 14-pods Cu<sub>2</sub>O frameworks were first formed. Through understanding the effect of solvent on the branching growth of Cu<sub>2</sub>O microcrystals, the habit growth can be independently controlled and the ability to control the morphology of Cu<sub>2</sub>O microcrystals can be achieved. In recent years, the studies using Cu<sub>2</sub>O crystals as sacrificial templates for the formation of Cu<sub>x</sub>S hollow architectures have attracted increasing interests.<sup>30–35</sup> Compared with other templates, Cu<sub>2</sub>O crystals have many special advantages, such as easily controlled structures, cost saving, multiple morphology, and convenient large-scale production.<sup>36,37</sup> Herein, a template-assisted synthesis of multipod frameworks of Cu<sub>7</sub>S<sub>4</sub> microcages using the obtained Cu<sub>2</sub>O microcrystals as sacrificial templates is reported. Hollow Cu<sub>7</sub>S<sub>4</sub> microcages were obtained in three steps involving the synthesis of Cu<sub>2</sub>O crystals with different morphologies, the formation of Cu<sub>2</sub>O/Cu<sub>7</sub>S<sub>4</sub> core/shell structures in Na<sub>2</sub>S ethanol and aqueous mixed solution, and the dissolution of the inner Cu<sub>2</sub>O cores in ammonia solution. Details of the experiments are provided in Supporting Information.

Figures 1a, b present typical scanning electron microscopy (SEM) images of the 14-pods Cu<sub>2</sub>O prepared in a medium of n-butyl alcohol/water at a volume ratio of 3.2: 6.8. The detailed structures of Cu<sub>2</sub>O microcrystal particles are shown in high-magnified SEM images. The sizes of the 14-pods Cu<sub>2</sub>O typically range from 10 to 15  $\mu$ m, with an average branching length of  $\sim$ 5  $\mu$ m. This type of multipod framework has fourteen uniform branching: along 6  $\langle 100 \rangle$  directions and along 8  $\langle 111 \rangle$  directions. They are marked as type II 14-pods Cu<sub>2</sub>O in this work. Through the reaction of these 14-pods Cu<sub>2</sub>O with a mixed ethanol and aqueous Na<sub>2</sub>S solution at 0  $^{\circ}$ C in air, followed by dissolution of the Cu<sub>2</sub>O cores in ammonia solutions, 14-pods Cu<sub>7</sub>S<sub>4</sub> cages with uniform morphologies similar to those of the Cu<sub>2</sub>O templates were obtained (Figure 1c). Inset of (c) is the high magnification image of a broken 14-pods Cu<sub>7</sub>S<sub>4</sub> cage, which clearly shows a hollow interior. The branching of a broken 14-pods Cu<sub>7</sub>S<sub>4</sub> cage is shown in high-magnified SEM images (Figure 1e), which indicates microcages with a wall thickness of about 50 nm. The detailed structure of individual 14-pods Cu<sub>7</sub>S<sub>4</sub> cage is shown in high-magnified SEM images (Figure 1c), which clearly indicates the

14-pods  $\text{Cu}_7\text{S}_4$  cages have a smooth surface. The morphology and interior structure of the 14-pods  $\text{Cu}_7\text{S}_4$  cages are further investigated by transmission electron microscopy (TEM).



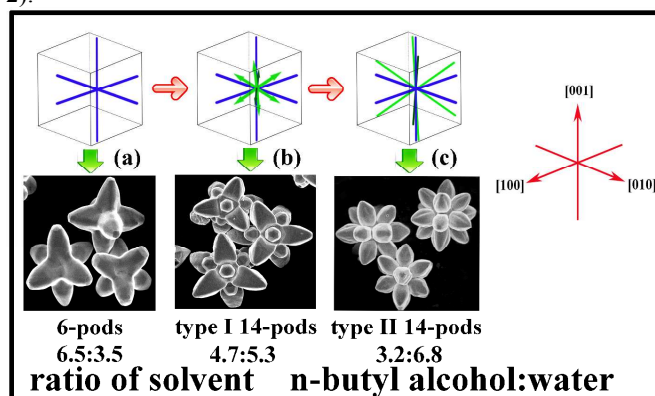
**Figure 1.** SEM images of a, b) 14-pods  $\text{Cu}_2\text{O}$ , and c, e) 14-pods  $\text{Cu}_7\text{S}_4$  cages. Inset of (a) is the high magnification image of 14-pods  $\text{Cu}_2\text{O}$ . Inset of (c) is the high magnification image of a broken 14-pods  $\text{Cu}_7\text{S}_4$  cage. d) SEM images of a branch of the broken 14-pods  $\text{Cu}_7\text{S}_4$  cage. f) TEM images of 14-pods  $\text{Cu}_7\text{S}_4$  cages. The 14-pods  $\text{Cu}_7\text{S}_4$  cages were prepared by reaction of the 14-pods  $\text{Cu}_2\text{O}$  precursor crystals shown in (a) with  $\text{Na}_2\text{S}$  solution at 0 °C in air followed by dissolution in ammonia solution.

Figure 1f shows that the particle has a regular 14-pods shape and a strong contrast between their edges (dark) and centers (bright), which also indicates microcages with a hollow interior. It has been reported that the crystal shape is determined by two growth processes: habit formation and branching growth.<sup>38–43</sup> Crystal habit is determined by the relative order of surface energies of different crystallographic planes of a crystal.<sup>38,39</sup> Branching growth is created by the diffusion effect.<sup>40,41</sup> When a crystal grows, ions or molecules near the surface are taking up by the growing crystal and a concentric diffusion field forms around the crystal.<sup>42,43</sup> This process forms the apexes of a polyhedral crystal, which protrude further into the region of higher concentration and grow faster than the central parts of facets, thus forming branches. The branching growth, however, generates rough and unstable surfaces that have many surface dangling bonds. The surface dangling bonds can rapidly

increase the growth kinetic coefficient in these regions and compensate for the diffusion effect, resulting in faceting growth to form flat and smooth faces.<sup>40, 41</sup> Therefore, preference for branching and faceting growth can be altered by growth conditions that amplify or minimize the diffusion effect.

X-ray diffraction (XRD) analysis was used to determine the phases of the pure  $\text{Cu}_2\text{O}$  microcrystals and the hollow  $\text{Cu}_7\text{S}_4$  microcages (Figure S1–S3). Figure S1c shows the XRD pattern of the as-prepared type II 14-pods  $\text{Cu}_2\text{O}$ . All the diffraction peaks are labeled and can be indexed according to the cubic phase of  $\text{Cu}_2\text{O}$  with PDF file No. 05-0667 (Figure S1a). No peaks from impurities such as  $\text{CuO}$  and  $\text{Cu}$  were observed. Figure S1d shows the XRD pattern of type II the 14-pods hollow  $\text{Cu}_7\text{S}_4$  formed by reaction of the 14-pods  $\text{Cu}_2\text{O}$  with  $\text{Na}_2\text{S}$  solution in air. The pattern of the obtained type II 14-pods cages is consistent with the standard spectrum of monoclinic  $\text{Cu}_7\text{S}_4$  with PDF file No. 23-0598 as shown in Figure S1b.

Our crystal growth experiments clearly showed that the branching was extremely sensitive to the chemical environment which in turn determined the final crystal morphology. In Figure 2, major branching patterns and the whole shape evolution of  $\text{Cu}_2\text{O}$  microcrystals from 6-pod frameworks to 14-pod frameworks of  $\text{Cu}_2\text{O}$  are presented as a function of solvent composition. The volume ratio of n-butyl alcohol to water in the reaction solvent played a crucial role in directing the overall morphologies of these intermediate structures. Under the n-butyl alcohol/water volume ratio of 6.5:3.5,  $\text{Cu}_2\text{O}$  crystal branching took place along all orientations of  $\langle 100 \rangle$ , which resulted in the formation of 6-pod frameworks (type (a), Figure 2).



**Figure 2.** A flowchart summary of various types of branching fashions (inset indicates the coordinate system) and corresponding SEM images of  $\text{Cu}_2\text{O}$  microcrystals under the current synthetic conditions: (a) six branching along  $\langle 100 \rangle$  directions; (b) six branching along  $\langle 100 \rangle$  directions and eight shorter branching along  $\langle 111 \rangle$  directions; and (c) six branching along  $\langle 100 \rangle$  directions and eight shorter branching along  $\langle 111 \rangle$  directions. Colored lines within a cubic box are equivalent; they are used to enhance the visibility.

It is interesting to note that with the decrease of volume ratio of n-butyl alcohol/water, a new type of multipod framework emerged (type (b), Figure 2). This type of multipod framework showed fourteen branching: six branching along  $\langle 100 \rangle$  directions and eight shorter branching along  $\langle 111 \rangle$  directions. With further decrease of the n-butyl alcohol/water volume ratio to 3.2:6.8, the branching along  $\langle 111 \rangle$  directions was gradually grown, finally leading to the formation of type II 14-pods  $\text{Cu}_2\text{O}$

with fourteen uniform branching: 6 along  $\langle 100 \rangle$  directions and 8 along  $\langle 111 \rangle$  directions (type (c), Figure 2). With further decrease of the n-butyl alcohol/water volume ratio to 0:10, the branching along  $\langle 111 \rangle$  directions was gradually grown, finally leading to the formation of 8-pods  $\text{Cu}_2\text{O}$  with eight uniform branching  $\langle 111 \rangle$  directions (Figure S4). Therefore, it seems that n-butyl alcohol selectively adsorbs onto the (111) surface of  $\text{Cu}_2\text{O}$  which hinders its further growth.

Figure 3a shows a typical SEM image of the 14-pods  $\text{Cu}_2\text{O}$  prepared in a solvent of n-butyl alcohol/water at a volume ratio of 4.7: 5.3. The detailed structure of a  $\text{Cu}_2\text{O}$  microcrystal particle is shown in high-magnified SEM image (Inset of (a)). The sizes of the 14-pods  $\text{Cu}_2\text{O}$  typically ranged from 10 to 15  $\mu\text{m}$ , with an average branching length of  $\sim 5 \mu\text{m}$ . This type of multipod framework has fourteen branching: six branching along  $\langle 100 \rangle$  directions and eight shorter branching along  $\langle 111 \rangle$  directions. They are marked as type I 14-pods  $\text{Cu}_2\text{O}$  in this work. The corresponding hollow 14-pods  $\text{Cu}_7\text{S}_4$  cages also exhibit uniform regular 14-pods morphology with smooth surfaces (Figure 3b,c). A typical TEM image of the 14-pods  $\text{Cu}_7\text{S}_4$  cage (Figure 3d) shows a perfect interior with a wall thickness of about 50 nm.

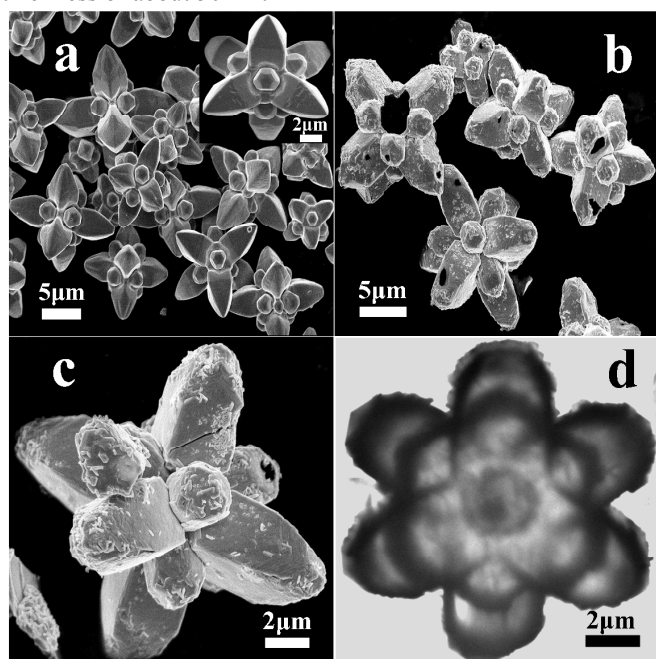
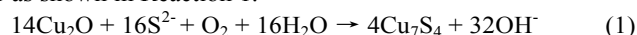


**Figure 3.** SEM images of a) 14-pods  $\text{Cu}_2\text{O}$ , and b,c) 14-pods  $\text{Cu}_7\text{S}_4$  cages. Inset of (a) is the high magnification image of 14-pods  $\text{Cu}_2\text{O}$ . d) TEM images of 14-pods  $\text{Cu}_7\text{S}_4$  cages.

Figure 4a shows a typical SEM image of the 6-pods  $\text{Cu}_2\text{O}$  prepared in a medium of n-butyl alcohol/water at a volume ratio of 3.2: 6.8. The detailed structure of a  $\text{Cu}_2\text{O}$  microcrystal particle is shown in high-magnified SEM image (Inset of (a)). This type of multipod framework showed six uniform branching along  $\langle 100 \rangle$  directions. Figure 4b-d show typical SEM and TEM images of a hollow  $\text{Cu}_7\text{S}_4$  that was formed against the 6-pods  $\text{Cu}_2\text{O}$  crystal, which clearly indicates a hollow 6-pods structure.

The formation of hollow  $\text{Cu}_7\text{S}_4$  microcages was the result of the small solubility product constant  $K_{\text{sp}}$  of copper sulfide ( $K_{\text{sp}}$

$\approx 10^{-48}$ ).  $\text{Cu}_2\text{O}$  particles suspended in the  $\text{Na}_2\text{S}$  solution were immediately converted into  $\text{Cu}_2\text{O}/\text{Cu}_7\text{S}_4$  core/shell structures in air as shown in Reaction 1.



The formation of the  $\text{Cu}_2\text{O}/\text{Cu}_7\text{S}_4$  core/shell structures can be considered as the Kirkendall effect.<sup>44</sup> In this approach, the specific  $\text{Cu}_2\text{O}$  structure allows diffusion of copper (I) ions from the central region to the surface and  $\text{Cu}_7\text{S}_4$  was produced there at first.  $\text{Cu}_2\text{O}/\text{Cu}_7\text{S}_4$  core/shell particles with cracked shells were formed. After dissolving the  $\text{Cu}_2\text{O}$  core in ammonia solution according to Reaction 2, hollow  $\text{Cu}_7\text{S}_4$  microcages were obtained.<sup>26</sup>

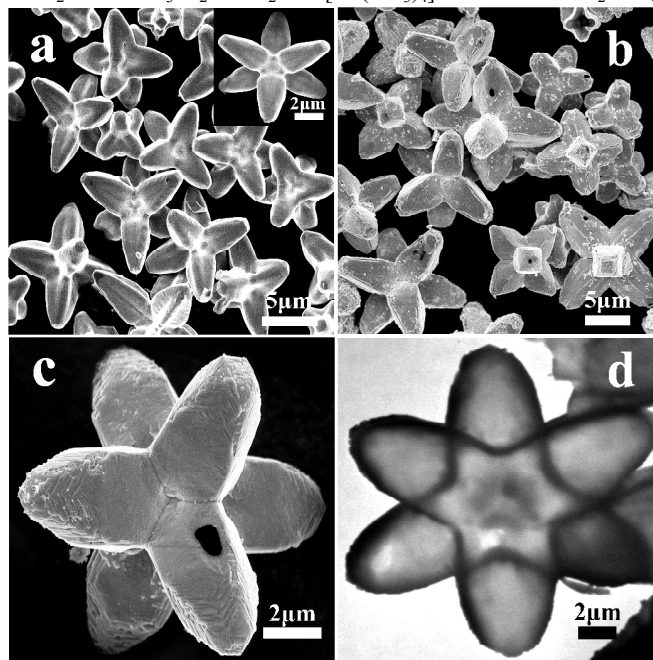
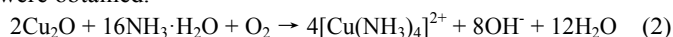


**Figure 4.** SEM images of a) 6-pods  $\text{Cu}_2\text{O}$ , and b,c) 6-pods  $\text{Cu}_7\text{S}_4$  cages. Inset of (a) is the high magnification image of 6-pods  $\text{Cu}_2\text{O}$ . d) TEM images of 6-pods  $\text{Cu}_7\text{S}_4$  cages.

## Conclusions

In summary, a variety of multipod frameworks of  $\text{Cu}_2\text{O}$  microcrystals have been prepared through careful control of the volume ratios of n-butyl alcohol to water in the reaction solvent. In particular, 14-pods  $\text{Cu}_2\text{O}$  frameworks were first prepared. These results provide a facile procedure for the controlled preparation of novel multi-morphologic  $\text{Cu}_2\text{O}$  microcrystals. Moreover, a template-assisted synthesis of multipod frameworks of  $\text{Cu}_7\text{S}_4$  microcages using the obtained  $\text{Cu}_2\text{O}$  microcrystals as sacrificial templates was established. This study revealed an important strategy in the design, controlled crystal growth, and morphology-controlled synthesis of multipod frameworks of  $\text{Cu}_2\text{O}$  microcrystals and  $\text{Cu}_7\text{S}_4$  microcages. It will also promote the synthesis and application of other inorganic building blocks.

## Acknowledgements

This work was supported by the National Natural Science Foundation of China (No.21271082, 21301066 and 21371068).

## Notes and references

<sup>a</sup>State Key Laboratory of Inorganic Synthesis and Preparative Chemistry, College of Chemistry, Jilin University, 2699 Qianjin Street, Changchun 130012, P. R. China. Fax: (+86) 431-85168316; Tel: (+86) 431-85168316. E-mail: [liucy@jlu.edu.cn](mailto:liucy@jlu.edu.cn).

<sup>b</sup> College of earth science, Jilin University, Changchun 130061, P. R. China.

<sup>c</sup>School of Chemistry and Chemical Engineering, Hainan Normal University, Haikou, 571158, P. R. China

† Electronic Supplementary Information (ESI) available: Experimental section and the XRD of products obtained at different reaction conditions (Figure S1-S3).

See DOI: 10.1039/c000000x/

- 1 C. Burda, X. B. Chen, R. Narayanan and M. A. El-Sayed, *Chem.ReV.*, 2005, **105**, 1025.
- 2 T. Haxhimali, A. Karma, F. Gonzales and M. Rappaz, *Nat. Mater.*, 2006, **5**, 660.
- 3 S. Lee, Y. Jun, S. Cho and J. Cheon, *J. Am. Chem. Soc.*, 2002, **124**, 11244.
- 4 N. Zhao and L. Qi, *Adv. Mater.*, 2006, **18**, 359.
- 5 D. Wang, D. B. Yu, M. W. Shao, X. M. Liu, W. C. Yu and Y. T. Qian, *J. Cryst. Growth*, 2003, **257**, 384.
- 6 D. Zitoun, N. Pinna, N. Frolet and C. Belin, *J. Am. Chem. Soc.*, 2005, **127**, 15034.
- 7 X. Zhong, R. Xie, L. Sun, I. Lieberwirth and W. Knoll, *J. Phys. Chem. B*, 2006, **110**, 2.
- 8 T. Ould-Ely, D. Prieto-Centurion, A. Kumar, W. Guo, W. V. Knowles, S. Asokan, M. S. Wong, I. Rusakova, A. Luttge and K. H. Whitmire, *Chem. Mater.*, 2006, **18**, 1821.
- 9 B. J. Murray, Q. Li, J. T. Newberg, E. J. Menke, J. C. Hemminger and R. M. Penner, *Nano Lett.*, 2005, **5**, 2319.
- 10 Y. Chang, and H. C. Zeng, *Cryst. Growth Des.*, 2004, **4**, 273.
- 11 (a) Z. H. Liang and Y. J. Zhu, *Mater. Lett.*, 2005, **59**, 2423. (b) J. S. Xu, D. F. Xue, *Acta Mater.*, 2007, **55**, 2397.
- 12 X. Zhang, Y. Xie, F. Xu, D. Xu and H. Liu, *Can. J. Chem.*, 2004, **82**, 1341.
- 13 C. W. Bunn, *Discuss. Faraday Soc.*, 1949, **5**, 132 – 144.
- 14 A. O. Musa, T. Akomolafe and M. J. Carter, *Sol. Energy Mater. Sol. Cells.*, 1998, **51**, 305.
- 15 P. Poizot, S. Laruelle, S. Grugeon, L. Dupont and J. M. Tarascon, *Nature*, 2000, **407**, 496.
- 16 J. T. Zhang, J. F. Liu, Q. Peng, X. Wang and Y. D. Li, *Chem. Mater.*, 2006, **18**, 867.
- 17 C. H. Kuo and M. H. Huang, *J. Am. Chem. Soc.*, 2008, **130**, 12815.
- 18 W. C. Huang, L. M. Lyu, Y. C. Yang and M. H. Huang, *J. Am. Chem. Soc.*, 2012, **134**, 1261.
- 19 J. Y. Ho and M. H. Huang, *J. Phys. Chem. C*, 2009, **113**, 14159.
- 20 C. H. Kuo, C. H. Chen and M. H. Huang, *Adv. Funct. Mater.*, 2007, **17**, 3773.
- 21 M. J. Siegfried and K.-S. Choi, *Adv. Mater.*, 2004, **16**, 1743-1746.
- 22 M. J. Siegfried and K.-S. Choi, *Angew. Chem., Int. Ed.*, 2005, **44**, 3218.
- 23 X. Zhang, Y. Xie, F. Xu, D. Xu and H. Liu, *Can. J. Chem.*, 2004, **82**, 1341.
- 24 Y. Chang and H. C. Zeng, *Cryst. Growth Des.*, 2004, **4**, 273.
- 25 J. S. Xu and D. F. Xue, *Acta Mater.*, 2007, **55**, 2397.
- 26 Y.-S. Cho and Y.-D. Huh, *Bull. Korean Chem. Soc.*, 2014, **35**, 309.
- 27 G. Prabhakaran and R. Murugan, *CrystEngComm.*, 2012, **14**, 8338.
- 28 Y. M. Sui, W. Y. Fu, H. B. Yang, Y. Zeng, Y. Y. Zhang, Q. Zhao, Y. G. Li, X. M. Zhou, Y. Leng, M. H. Li and G. T. Zou, *Cryst. Growth Des.*, 2010, **10**, 99.
- 29 K. F. Chen, C. T. Sun and D. F. Xue, *Phys. Chem. Chem. Phys.* 2015, **17**, 732.
- 30 S.H. Jiao, L.F. Xu, K. Jiang, and D.S. Xu, *Adv. Mater.*, 2006, **18**, 1174-1177.
- 31 S. D. Sun and Z. M. Yang, *ChemComm*, 2014, **50**, 7403.
- 32 (a) S. D. Sun, X. P. Song, C. C. Kong, S. H. Liang, B. J. Ding and Z. M. Yang, *CrystEngComm*, 2011, **13**, 6200. (b) S. D. Sun, X. P. Song, C. C. Kong, D. C. Deng and Z. M. Yang, *CrystEngComm*, 2012, **14**, 67.
- 33 W. X. Zhang, Z. X. Chen and Z. H. Yang, *Phys. Chem. Chem. Phys.*, 2009, **11**, 6263.
- 34 S. D. Sun, S. Wang, D. C. Deng and Z. M. Yang, *New J. Chem.*, 2013, **37**, 3679.
- 35 G. X. Chen, M. T. Niu, L. F. Cui, F. Bao, L. H. Zhou, and Y. S. Wang, *J. Phys. Chem. C*, 2009, **113**, 7522.
- 36 M. Leng, C. Yu and C. Wang, *CrystEngComm*, 2012, **14**, 8454.
- 37 C. H. Kuo and M. H. Huang, *Nano Today*, 2010, **5**, 106–116.
- 38 (a) M. J. Siegfried and K. S. Choi, *Angew. Chem., Int. Ed.*, 2005, **44**, 3218. (b) F. Sun, Y. P. Guo, Y. M. Tian, J. D. Zhang, X. T. Lv, M. G. Li, Y. H. Zheng and Z. C. Wang, *J. Cryst. Growth.*, 2008, **310**, 318.
- 39 M. J. Siegfried and K. S. Choi, *Adv. Mater.*, 2004, **16**, 1743.
- 40 W. B. Floriano and M. A. C. Nascimento, *Braz. J. Phys.*, 2004, **34**, 38.
- 41 A. A. Chernov, *J. Cryst. Growth*, 1974, **24/25**, 11 – 31.
- 42 T. Kudora, T. Irisawa, A. Ookawa, *J. Cryst. Growth*, 1977, **42**, 41 – 46.
- 43 W. F. Berg, *Proc. R. Soc. London Ser. A*, 1938, **164**, 79 – 96.
- 44 M. Basu, A. K. Sinha, M. Pradhan, S. Sarkar, Govind and T. Pal, *J. Phys. Chem C*, 2011, **115**, 12275.



Synthesis and Characterization of Multipod Frameworks of Cu<sub>2</sub>O

Microcrystals and Cu<sub>7</sub>S<sub>4</sub> Hollow Microcages

Hongdan Zhang,<sup>a</sup> Ziqing Zhang,<sup>a</sup> Benxian Li,<sup>b</sup> Yingjie Hua<sup>c</sup> Chongtai Wang,<sup>c</sup> Xudong Zhao<sup>a\*</sup> and Xiaoyang Liu<sup>a\*</sup>

The 14-pods Cu<sub>2</sub>O frameworks are first prepared through control of the ratios of n-butyl alcohol to water.

